

Impact of surface strain on the spin dynamics of deposited Co nanowires

O. P. Polyakov,^{1,a)} J. G. Korobova,^{1,a),b)} O. V. Stepanyuk,² and D. I. Bazhanov^{1,2,3}

¹*Faculty of Physics, Moscow State University, Leninskiye Gory, 1, Building 2, Moscow 119991, Russia*

²*Institution of Russian Academy of Sciences, Dorodnicyn Computing Centre of RAS, Vavilov St. 40, 119333 Moscow, Russia*

³*Max-Planck Institut für Mikrostrukturphysik, Weinberg 2, D-06120 Halle, Germany*

(Received 22 August 2016; accepted 15 December 2016; published online 3 January 2017)

Tailoring the magnetic properties at atomic-scale is essential in the engineering of modern spintronics devices. One of the main concerns in the novel nanostructured materials design is the decrease of the paid energy in the way of functioning, but allowing to switch between different magnetic states with a relative low-cost energy at the same time. Magnetic anisotropy (MA) energy defines the stability of a spin in the preferred direction and is a fundamental variable in magnetization switching processes. Transition-metal wires are known to develop large, stable spin and orbital magnetic moments together with MA energies that are orders of magnitude larger than in the corresponding solids. Different ways of controlling the MA have been exploited such as alloying, surface charging, and external electrical fields. Here we investigate from a first-principle approach together with dynamic calculations, the surface strain driven mechanism to tune the magnetic properties of deposited nanowires. We consider as a prototype system, the monoatomic Co wires deposited on strained Pt(111) and Au(111) surfaces. Our first-principles calculations reveal a monotonic increase/decrease of MA energy under compressive/tensile strain in supported Co wire. Moreover, the spin dynamics studies based on solving the Landau-Lifshitz-Gilbert equation show that the induced surface-strain leads to a substantial decrease of the required external magnetic field magnitude for magnetization switching in Co wire. *Published by AIP Publishing.* [<http://dx.doi.org/10.1063/1.4973366>]

I. INTRODUCTION

Creation of modern technological applications, such as high-density magnetic recording and memory storage devices, demands systems with a high value of magnetic anisotropy (MA) energy.¹ Basically, the MA determines the orientation of the magnetization with respect to the lattice structure and the stability of the magnetization direction. High MA energy provides the stability of a certain magnetic state upon thermal fluctuations, external field exposure, or electric currents. On the other hand, magnetic memory recording devices design demands to pursuit conditions, where one can induce magnetization-switching with relative low-cost energy. Both conditions are essential issues for future nanostructures engineering. In order to get a thorough-going understanding regarding the details of the physical processes which take place in real magnetic nanostructures, the study of their underlying spin-dynamics is fundamental. Recently, atomistic spin-dynamics simulations in supported monoatomic finite chains regarding spontaneous magnetization reversal processes with inclusion of the thermal fluctuations have been carried out.² It was shown that the magnetization lifetime depends on the length of the chain. The evolution in time of the magnetization strongly depends on the MA energy and spin magnetic moments of a system. Very often, a decrease of dimensionality directly leads to an enhancement of MA energy. In this context, low-dimensional structures such as metallic nanowires are of a great interest in modern research.¹ After the experimental demonstration regarding the possibility of

growing ordered arrays of monoatomic Co chains on Pt(997) surface with a precise coverage,³ numerous studies of deposited nanowires and their magnetic properties^{4–10} were reported. Further studies revealed a ferromagnetic state in monoatomic cobalt chains on the Pt(997) surface exhibiting enhanced orbital moments and MA energy in comparison to the two-dimensional films or bulk systems.¹¹ Numerous studies reported that *3d-5d* transition metal wires develop a large, stable spin, and orbital magnetic moments and MA energies significantly larger than in their corresponding solids.^{1,12,13} In this context, the fact of being able to control and tune the magnetic properties of *3d-5d* metal nanostructures at the atomic level opens new routes for building nanostructures with specific functionalities and better performance.

The structural effects have also an impact on the magnetic properties of nanostructures. It is well-known, that the equilibrium bond length changes with the dimensionality and coordination number. For instance, the reduction of the bond length of the atoms in a crystal surface leads to the appearance of an in-plane stress. This strain can favor the reconstruction of the surface in order to minimize its surface energy. This effect is known as a mesoscopic misfit¹⁴—deformations of the surface and the nanostructures thereon induced by a multitude of effects connected with the finite size of the system or the inherent mismatch of lattice constants of different materials. Stress can cause large modifications in the electronic and magnetic properties of nanostructures, because even inconspicuous structural changes can play a crucial role at atomic distances. During the film epitaxial growth,^{15,16} a surface-strain is induced due to mismatch of lattice constants between the deposited structure

^{a)}O. P. Polyakov and J. G. Korobova contributed equally to this work.

^{b)}Electronic mail: korobovajg@gmail.com

and the surface of the substrate. The changing of electronic^{14,17} and magnetic^{14,18,19} properties under strain has been largely observed in film systems, and it is employed in order to alter their physical properties. For instance, recent direct magnetization measurements in a 20 nm thick (Ga,MN)As layer deposited on (Ga,In)As buffer with very large epitaxial strains have demonstrated the linear dependence of the MA as a function of the stress strength.²⁰ Recently, it was shown from the first principles that applying of 10% biaxial tensile strain to phthalocyanine sheets decorated by 5*d* transition metals such as Os and Ir leads to the significant enhancement of MA energy up to 140 meV.²¹ Also, the first-principles study demonstrated that MA of bulk FePt can be altered significantly by a moderate applied biaxial strain and the MA energy decreases under the action of tensile strain in such system.²² Moreover, the usage of strained surface as a template can lead to the change of the diffusion barriers in adsorbed adatoms.²³ Surface-strain can also affect the electrical properties of transition metals by changing the work-function of the metal-terminated carbide surfaces and their band structure.²⁴ It has been shown that the epitaxial strain can vary the *d*-states filling and their degeneracy^{20,25–29} and also can modify the transport and magnetic properties of the nanostructures.³⁰

Therefore, it is very intriguing to apply the surface strain as a tool for deposition of metal nanowires. It can lead to the onset of strained nanowires with modified physical properties. Those wires will have different interatomic distances in comparison to the ones deposited onto non-strained substrates. Consequently, this interatomic distance difference in the wires induces profound effects on the electronic and magnetic properties, in particular, the MA. Recently, the experimental study revealed the growth of uni-dimensional Co chains on uni-axially strained Au(111) surfaces.³¹ This experimental work provides a direct evidence that the monoatomic nanowires can also exist on strained surfaces.

In this case, the employment of strained surfaces as templates for wire deposition can affect the magnetization dynamics of the deposited nanowires opening a manner for tailoring magnetization switching processes. In this work, our main goal is to study the impact of surface strain on magnetic properties and their underlying magnetization dynamics of deposited metallic one-dimensional (1D) wires taking Co wires deposited on strained Pt(111) and Au(111) as examples. We show for these nanowires that surface stretching can monotonically decrease the magnetic anisotropy energy and can significantly reduce the magnitude of the external magnetic field required for magnetization switching.

II. THEORETICAL BACKGROUND

We considered infinitely long (one-dimensional (1D)) ferromagnetically coupled Co wires placed on Pt(111) and Au(111) surfaces along [010] direction (*y* axis) following an epitaxial *fcc*-adsorption growth and having a lattice parameter *a* within a surface unit cell. Our first-principles study is carried out in the framework of the density functional theory using the projector augmented wave technique³² as it is implemented in the VASP (Vienna ab initio Simulation

Package) code.³³ The Kohn-Sham equations⁵⁵ are solved within a supercell approach considering the periodic boundary conditions and a plane-wave basis set. The supercell dimension in the broken-symmetry direction [001] (*z*-axis) is chosen large enough (typically 15 Å) so as to avoid any spurious interactions between the periodic replicas. The electron exchange and correlation effects have been taken into account using the generalized gradient approximation (GGA, PW91).³² A maximal kinetic energy cutoff of 500 eV is employed. The integration over the Brillouin zone consistent with the geometry of our system has been performed using the Monkhorst-Pack scheme⁵⁶ with a *k*-mesh of $6 \times 24 \times 1$. Structural relaxations are achieved using the quasi-Newton algorithm. Relaxations were performed until forces acting on each ion became less than 0.01 eV/Å. We found that the chosen parameters provide enough reliability in the accuracy of the present calculations.³⁴ Dipole-dipole interactions and the corresponding associated anisotropy are ignored, since this kind of anisotropy is mainly attributed to the long-range interactions. It is significantly smaller than the magneto-crystalline anisotropy where the short-range interactions dominate such as in the case of adatoms or nanowires deposited on highly polarizable substrates.^{35,36}

As a first step, we determine the equilibrium bulk lattice parameter *a*₀ performing self-consistent calculations including atomic relaxations. The obtained values are 4.17 Å and 3.99 Å for the Au and Pt surfaces, respectively. In order to investigate the impact of the strain on the magnetic properties of 1D-wires, we introduce a tensile and compressive surface strain to the system by stretching or shrinking uniformly the surface unit cell relative to its equilibrium lattice parameter. For instance, such surface stress can be induced during pseudomorphic growth of thin metal films in heteroepitaxy processes.²⁰ For both considered substrates, we use a six-layer model-slab keeping the three bottom layers fixed with the aim of taking into account the bulk and the surface states. As a second step, we performed non-relativistic calculations with a convergence criterion for the electronic energy of 10⁻⁷ eV/atom allowing the first three upper layers to relax together with the wire atoms adequately permitting to take into account the substrate-wire interactions and the substrate hybridizations as is the case in the experiments.

Finally, relativistic calculations including spin-orbit coupling with the same energy criteria are carried out to calculate the MA energy of the wire-substrate system. For the sake of comparison, both self-consistent and non-self-consistent (magnetic force theorem) calculations were also performed to determine the possible discrepancies in the MA. In general, we found that both approaches yield to similar values of the MA energy. MA energies are defined as the difference between energies corresponded to the magnetization easy and hard axis directions.

In order to study the time-evolution of the magnetization of the nanowires, we employ the modified Landau-Lifshitz-Gilbert (LLG) equation. Despite its macroscopic origin, it has been shown that this equation is useful for studying the magnetization dynamics of nanostructures.^{37–41} The LLG equation adapted for atomic-scale systems can be written as⁴²

TABLE I. Local atomic structure of the Co wire on Au(111) surface with respect to the applied strain, where h —the height of Co-wire above the surface.

Latt. parameter (Å)	3.998	4.039	4.079	4.120	4.161	4.202
$h_{\text{Co-Au}}$ (Å)	1.934	1.937	1.880	1.840	1.781	1.708

$$\frac{\partial \mathbf{S}_i}{\partial t} = -\gamma \mathbf{S}_i \times \mathbf{H}_{\text{eff}}^i + \frac{\alpha}{\mu_s} \mathbf{S}_i \times \frac{\partial \mathbf{S}_i}{\partial t}, \quad (1)$$

where ($\mathbf{S}_i \equiv \boldsymbol{\mu}_s/\mu_s$) is a unit vector of the i -th atom magnetic spin moment, γ is the gyromagnetic ratio, μ_s the atomic spin moment, $\mathbf{H}_{\text{eff}}^i$ the effective magnetic field acting on the i -th atom and α is the damping parameter. In the atomic case, the α -parameter does not contain the macroscopic factors such as the demagnetization fields, temperature dependence, etc. In the framework of our study, the effective magnetic field involves the influence of external magnetic fields, uniaxial crystalline anisotropy, and exchange interaction

$$\mathbf{H}_{\text{eff}}^i = \frac{\partial}{\partial \mathbf{S}_i} \left[\mathbf{S}_i \mathbf{H} + \frac{K_i}{\mu_s} (\mathbf{S}_i \mathbf{e}_a)^2 + \sum_{j(j \neq i)} \frac{J_{ij}}{\mu_s} \mathbf{S}_i \mathbf{S}_j \right]. \quad (2)$$

Here J_{ij} is the exchange interaction between i -th and j -th atoms ($J_{ij} < 0$ for antiferromagnetic and $J_{ij} > 0$ for ferromagnetic couplings, respectively), K_i is the MA energy of i -th atom, \mathbf{e}_a denotes the direction of the easy magnetization axis. For the numerical resolution of the LLG equation, we use a home-made code based on the Runge-Kutta 4th order method with a time step of $\Delta t = 10^{-18}$ s.⁴³ We assigned a value for the damping parameter of $\alpha = 0.01$. These numbers are typical for such kind of dynamic calculations.^{44–48}

III. RESULTS AND DISCUSSION

First of all we investigated the surface-strain effects on the MA energy. The calculations show that both the types of induced strain (compressive and tensile) substantially modify the interlayer wire-substrate distance. Moreover, we found that for the case of Co wires deposited on Au(111), a steep surface strain larger than 6% with respect to the equilibrium lattice parameter, $|a| \geq a_0 \pm 6\%$, leads to a distortion of the wire-substrate system that completely changes the atomic structure of the surface and the (111)-symmetry is broken. We observe the formation of rows in the surface upon

TABLE II. Local atomic structure of the Co wire on Pt(111) surface with respect to the applied strain, where h —the height of Co-wire above the surface.

Latt. parameter (Å)	3.866	3.906	3.946	3.986	4.026	4.066	4.106
$h_{\text{Co-Pt}}$ (Å)	1.853	1.826	1.788	1.736	1.666	1.579	1.506

compression resembling the (001)-symmetry. A different behavior is seen when the system is under a tensile strain. In this case, the wires relax towards the substrate reducing the interlayer wire-substrate distance. Similar trends have been established during strain relief in a Co/Pt(111) system. Therefore, we have considered in our study only “moderate” strains up to $|a| \leq a_0 \pm 5\%$ where the symmetry of the substrate still remains. Even within this regime, the induced surface strain triggers noticeable structural effects. When the system is compressed, the interlayer substrate-wire distance monotonously increases 5% and 6% with respect to the unstrained structure for the Au(111) and Pt(111) substrates, respectively. Contrary, for the stretched system, this distance gradually reduces by 7% and 13% for considered surfaces, respectively. In Tables I and II, we present the interlayer substrate-wire distance h for several representative lattice parameters.

Since the geometrical environment is strongly related with the electronic structure, the Co d -orbitals hybridization provide insights regarding the microscopic origins of the structural effects. The change in the hybridization causes a redistribution of the Co d -states which are responsible for the magnetic properties of the 1D wires. Our analysis focuses on the states close to the Fermi energy which are the ones that mostly contribute to the MA behavior. First, we estimate the hybridization Δ_ν of the Co d -states for the considered systems. It was already shown⁴⁹ that the strength of coupling between the states in semiconductors and metals is entirely described by the quantity $\Delta_\nu(\epsilon)$, which has the dimension of energy. Therefore, we used the calculated electronic structure for the studying of the Co d -states hybridization between the neighboring atoms in the wire. The projected density of states (PDOS) $\rho_\nu(\epsilon)$ (Figs. 1(a) and 2(a)) was calculated in order to determine the hybridization Δ_ν (Figs. 1(b) and 2(b)) between state ν and surrounding atoms via the Kramers-Kronig relation,^{49,50} which is valid for any strength of the coupling

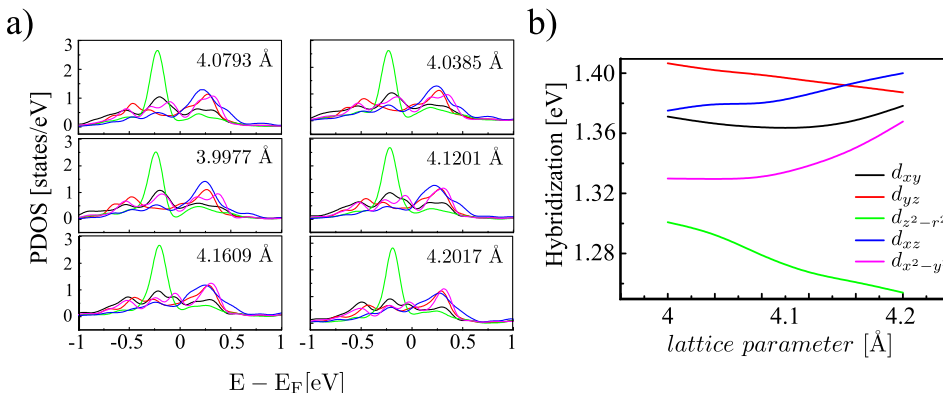
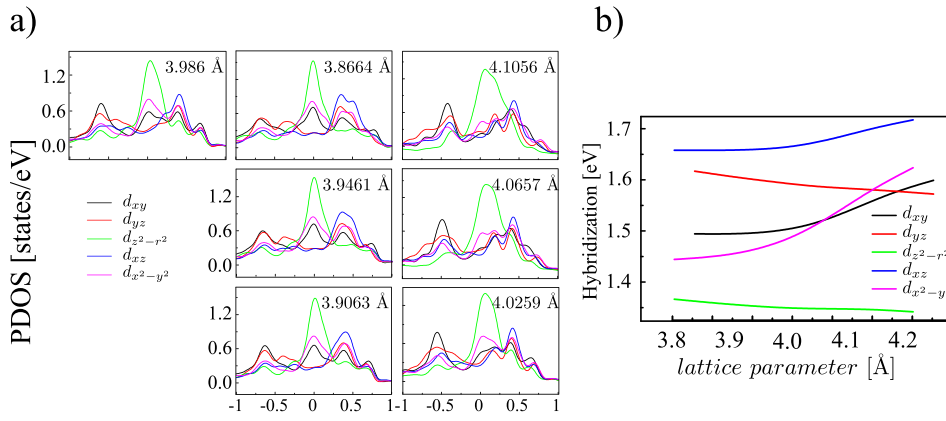


FIG. 1. (a) Calculated projected density of Co minority d -states $\rho_\nu(\epsilon)$ on a Au(111) substrate; (b) Hybridization Δ_ν determined from Eq. (3) at the Fermi energy as a function of substrate lattice parameter a .



$$\Delta_v(\epsilon) = -Im \left(\int_{-\infty}^{\infty} d\epsilon' \frac{\rho_v(\epsilon')}{\epsilon - \epsilon' - i0} \right)^{-1}. \quad (3)$$

The calculated PDOS for the Co/Au(111) system is presented in Fig. 1(a). Our calculations show that for all considered strains $d_{z^2-r^2}$ -state does not change its shape at the Fermi level. Thus, we can exclude this state from our analysis. As it can be appreciated in (Fig. 1(a)) during the transition from compressive strain to tensile one (to be referenced here as “surface stretching”) the role of $d_{x^2-y^2}$ increases, while d_{yz} maximum shifts to the unoccupied states. The hybridization of $d_{x^2-y^2}$ state strongly increases during surface stretching (Fig. 1(b)). Furthermore, in this case, the hybridizations of the d_{xy} and d_{xz} states are also increasing. Thus, we observe the increase of hybridization in supported 1D Co wire at the vicinity of the Fermi level with surface stretching. This result corresponds to the wire relaxation towards the substrate surface upon applying the tensile strain. For Co/Pt(111) system, the increase of Co d -states hybridization is also followed with the redistribution of atomic states at Fermi level. In this case, d_{yz} state does not change its shape at the Fermi level and, thereby, it will not be considered. The hybridization of the $d_{z^2-r^2}$ state insignificantly decreases with surface stretching, but its maximum shifts with tension to unoccupied states (Fig. 2(a)). Hybridization of d_{xy} , d_{xz} and $d_{x^2-y^2}$ states strongly increases with surface stretching, and they are rising at the Fermi level.

Consequently, we can conclude that the induced surface strain changes the electronic occupations of d -states close to the Fermi level and, as a result, it is expected to have a strong impact on the MA of deposited Co nanowires.

Now we turn to the discussion about the magnetic properties of deposited 1D Co wires. We investigated the dependence of total energy of the system as a function of the azimuthal (in-plane direction) and polar (out-of-plane direction) angles of magnetization. Here we present the detailed results for Co/Au(111) system (Fig. 3) as an example. Fig. 3 shows the total energy differences ($E(\phi) - E(90^\circ)$) and ($E(\theta) - E(90^\circ)$) (Fig. 3(a)) of Co/Au(111) system as a function of magnetization directions in in-plane and out-of-plane, expressed in terms of the angles, respectively. In order to estimate the MA energy, we have approximated the calculated total energy values by harmonic function $E(\alpha) - E(\alpha_{\min}) = C - E_{MA} \cos^2(\alpha + \alpha_{\min})$, where E_{MA} is the MA energy and α_{\min} is the magnetization easy axis direction (see curves in Fig. 3). Our results show that for all considered strains, magnetization easy axis favours in-plane direction. This result is in an agreement with the ones obtained for Co dimers and nanoclusters deposited on the Au(111) surface, where the in-plane anisotropy also was favorable.⁵¹ For the examined systems, we found that the MA energy decreases monotonically upon substrate stretching (Fig. 3(a)) in 2 times with respect to the value 0.46 meV, obtained for lattice parameter a_0 . Note, that the compressive strain of the substrate leads to the enhancement of MA energy. However, for this system, the magnetic moment of Co atoms in the wire does not change significantly with strain. It has a value around $1.99\mu_B$ over all considered strained wires.

The similar analysis of Co/Pt(111) revealed that the out-of-plane anisotropy is favorable for all considered strains. In the case of Co wires deposited on the Pt(111) surface, we observed a more significant decrease of the MA energy upon substrate stretching. It is 4 times lower with respect to the

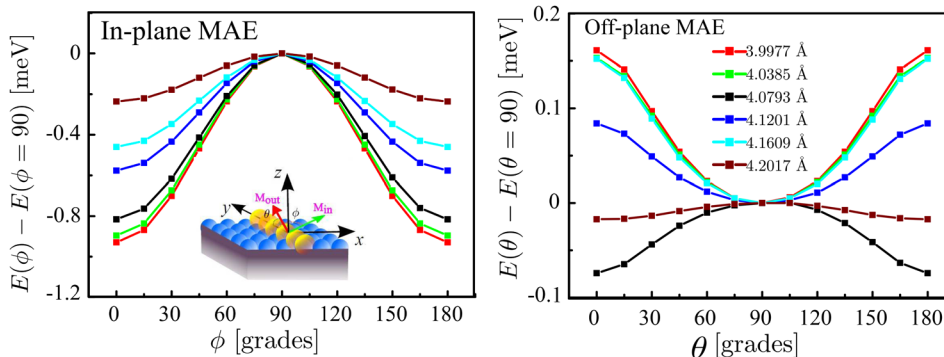


FIG. 3. Magnetization direction dependence of total energy (a) $E(\phi) - E(90^\circ)$ and (b) $E(\theta) - E(90^\circ)$, where ϕ and θ measures the angle as shown in the scheme in the figure and the MA energy value for different substrate lattice constants.

value 2.17 meV obtained for the lattice parameter a_0 . The magnetic moment of Co atoms in the wire has values around $2.1\mu_B$ for all considered strains. It is worth to note here, that in the case of Co/Pt(111) system, we observed a significant polarization of the substrate, while for the Au(111) surface, it was not such a case. This effect was understood through the weaker spin-orbit coupling between Co and Au atoms than in between the Co and Pt atoms. Test calculations including different number of layers in Pt substrate have not shown the changing of its polarization. Since a similar trend in the changing of the MA energy with surface strain is found for both systems, we conclude reasonably that the presence of substrate polarization does not play a key role in the behavior of MA energy. Polarization itself can make its own contribution to the magnitude of MA energy.

Consequently, we revealed that the increase of hybridization during relaxation of the Co 1D wire towards the substrate surface provoked by surface stretching is followed with the linear decrease of MA energy.

In order to obtain further insights regarding the MA behavior, we examined the density of d -states of Co atoms in the wire taking into account only the minority spin states, because the majority states are fully occupied in our system. The change of MA energy can be explained in terms of the second-order perturbation theory. The energy difference between two axes of quantization (y and z) can be written in the perturbation formula⁵²

$$\text{MA} = E_y - E_z \sim \xi^2 \sum_{o,u} \frac{|\langle \psi_u | l_z | \psi_o \rangle|^2 - |\langle \psi_u | l_y | \psi_o \rangle|^2}{\epsilon_u - \epsilon_o}, \quad (4)$$

where o and u specify the occupied and unoccupied minority spin states, respectively, l_y and l_z are the angular momentum operators. The parameter ξ is an average of spin-orbit coupling coefficients. This equation contains both the out-of-plane (first term) and in-plane (second term) contributions to the MA energy. The coupling between the occupied and unoccupied states around the Fermi level is very important and can largely affect the matrix elements of l_y and l_z . The interaction between the different couplings is the origin of the total magnetization direction. In summary, the total magnetization direction is strongly affected by the symmetry of the d -states via the couplings between them through the angular momentum operators, l_y and l_z approving an in-plane or out-of-plane MA (Table III).⁵²⁻⁵⁴

The orbital-projected local density of states for the Co atoms minority d -states in the systems Co/Au(111) and Co/Pt(111) are presented in Fig. 4.

TABLE III. Couplings between occupied and unoccupied states depending on the d -orbital symmetry and their contribution to the respective magnetization axis. The vertical (horizontal) arrows referred to an out-of-plane (in-plane) direction of magnetization.

$\langle \psi_u l \psi_o \rangle$	$d_{3z^2-r^2}$	$d_{x^2-y^2}$
d_{xy}	~ 0	\uparrow
d_{xz}	\rightarrow	\rightarrow
d_{yz}	\rightarrow	\rightarrow

It is well seen that the surface strain in the Co/Au(111) system leads to the shifting of $d_{3z^2-r^2}$ and d_{xy} maximums to the occupied states just below the Fermi level, while higher densities of d_{yz} and d_{xz} states are observed above the Fermi level. This d -states redistribution makes a strong effect on coupling through the angular momentum operators and changes the matrix elements in Eq. (4). After a careful analysis of local densities of states and matrix elements of the interaction between coupled states, we concluded that the dominant contribution to MA energy comes from coupling between occupied $d_{3z^2-y^2}$ and unoccupied d_{yz} and d_{xz} states. This contribution leads to the in-plane MA. The increase of $d_{3z^2-y^2}$ state upon applying of tensile strain (Fig. 4(a)) leads to the increase of its coupling with d_{yz} and d_{xz} states. As a result, we obtain the enhancement of in-plane contribution. Thus, the gap between in-plane and out-of-plane contributions to MA is decreased. This means the decrease of MA energy upon applying of tensile strain.

In the case of Co/Pt(111) system, applying of surface stretching to the system reduces the number of d_{xy} , $d_{3z^2-r^2}$ and $d_{x^2-y^2}$ states near the Fermi level, while the number of d_{yz} states increases (Fig. 4(b)). It enhances the coupling between $d_{3z^2-r^2}$ and d_{yz} states, which is responsible for in-plane anisotropy. However, the coupling between $d_{3z^2-r^2}$ and d_{xz} states weakens under the applied surface strain. Since this coupling also supports the in-plane anisotropy, its contribution to MA neutralises the contribution of $d_{3z^2-r^2}$ and d_{yz} coupling. It occurs owing to almost the same, but opposite, changing the number of d_{yz} and d_{xz} states at Fermi level during surface stretching. At the same time, the applied surface strain decreases the coupling between d_{xy} and $d_{x^2-y^2}$ states which is responsible for out-of-plane anisotropy. It is the most significant for the strained system and, thereon, is a driving force for the decreasing of MA energy and for the favoring of out-of-plane MA.

Next step we report our spin dynamics studies in supported Co nanowires. The spin dynamics of the deposited wires is investigated in the framework of the LLG theory. Local magnetic moments and anisotropy energies are taken from our first-principles calculations as parameters in the LLG equation of motion. Our aim is to study the impact of the induced strain on the magnetization switching processes.

The LLG equation is a stochastic equation of motion and usually huge computational resources are required in order to describe the evolution in time of the magnetization in systems containing a large number of atoms. However, within our approach for determining the magnetization dynamics, the computational efforts are significantly reduced. The interatomic exchange interaction decreases with the separation distance between the atoms, therefore we only take into account, the nearest-neighbor interactions in our analysis.³⁷ In our model, we consider the infinite ferromagnetic coupled chains of equivalent atoms, and the thermal fluctuations are neglected. Thus, our system can be seen as a set of atoms with equal magnetic moments and magnetic anisotropy (i.e., $\forall i, K_i = K, \mathbf{S}_i(0) = \mathbf{S}_0$) under an external applied magnetic field exposure with the same strength and direction (\mathbf{H}_{exc}). In this case, relying on Eqs. (1) and (2), each atom has an equivalent

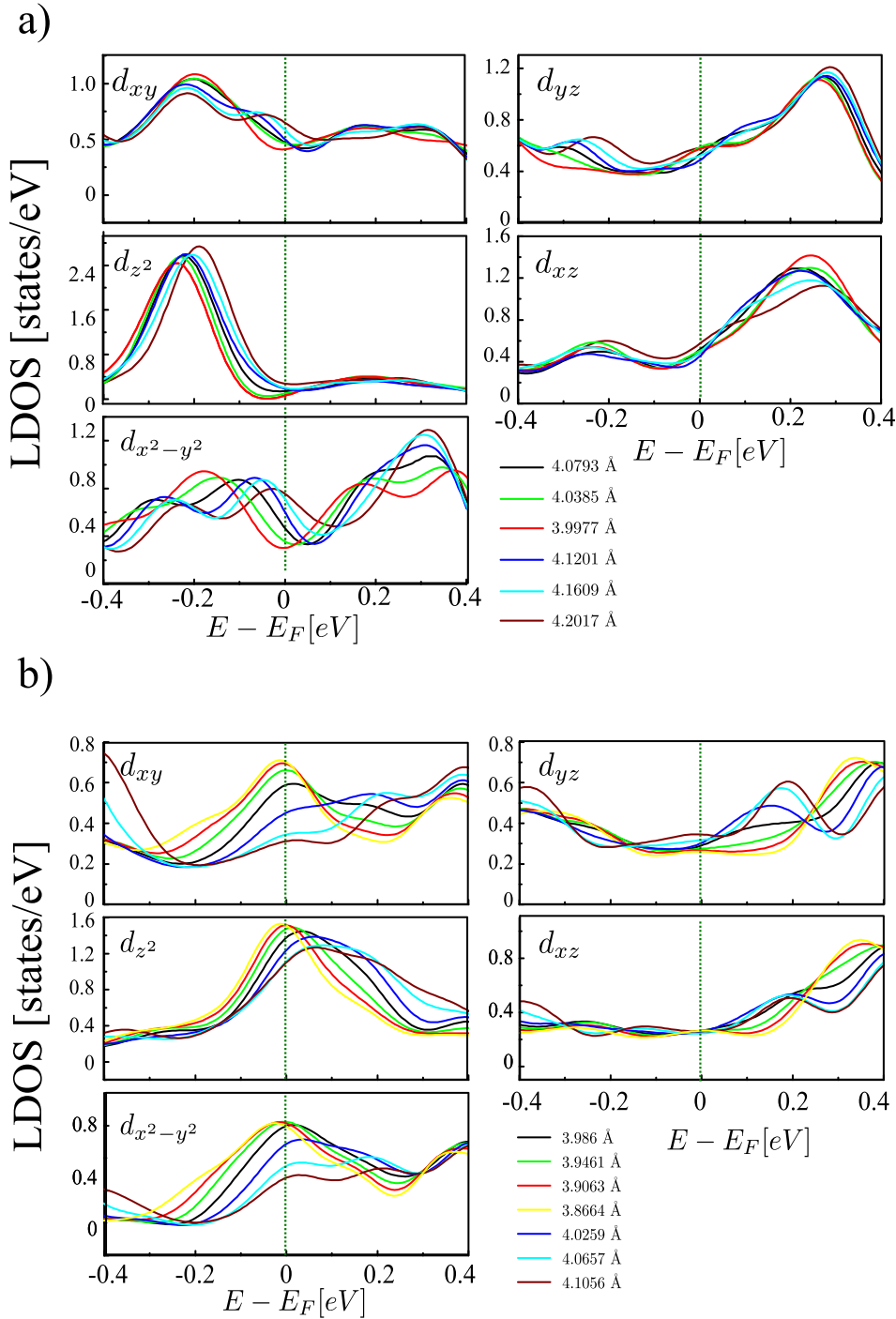


FIG. 4. (a) Orbital-projected local density of states for the minority d-states of Co atoms in the system Co/Au(111). (b) Orbital-projected local density of states for the minority d-states of Co atoms in the system Co/Pt(111). Density of majority states is negligibly small near the Fermi level.

spin dynamics implying the collinear spin rotations between the magnetization directions of the atoms as a function of the time t (or $\forall t, \mathcal{H}_{\text{exc}} = -\sum_{i \neq j} J_{ij} = \text{const}$). Consequently, in our case, the inter-atomic exchange interaction is not time-dependent. It means that in \mathcal{H}_{exc} , the time derivative should vanish. Thus, we can neglect the last term in Eq. (2) and simply describe the spin dynamics of the deposited ferromagnetic wires by analyzing the evolution of the magnetic behavior in time of only one atom.

For mere simplicity, we set the atom in the center of the Cartesian coordinate system and apply a constant magnetic field perpendicular to the wire, along the y -axis ($\mathbf{H} = H_y \mathbf{e}_y$). In this case, the magnetic ground state is parallel to the

direction of the magnetic field ($\Theta = \pi/2 + 2\pi m$, $\varphi = \pi/2 + 2\pi n$, $n, m \in \mathbb{Z}$) as it can be seen in Fig. 5.

Nevertheless, if an out-of-plane uniaxial anisotropy (i.e., the easy-axis of magnetization is along the z -direction) is taken into account in the model, a different spin dynamics is observed. In this case, the magnetization along the y -direction is not the groundstate anymore and two new stable magnetic states appear in the system

$$\begin{cases} \sin \Theta = \pm H_y \mu_s / 2K, \\ \cos \varphi = 0. \end{cases} \quad (5)$$

By starting the analysis with the Co/Pt(111) system, we determine from our first-principle calculations an anisotropy

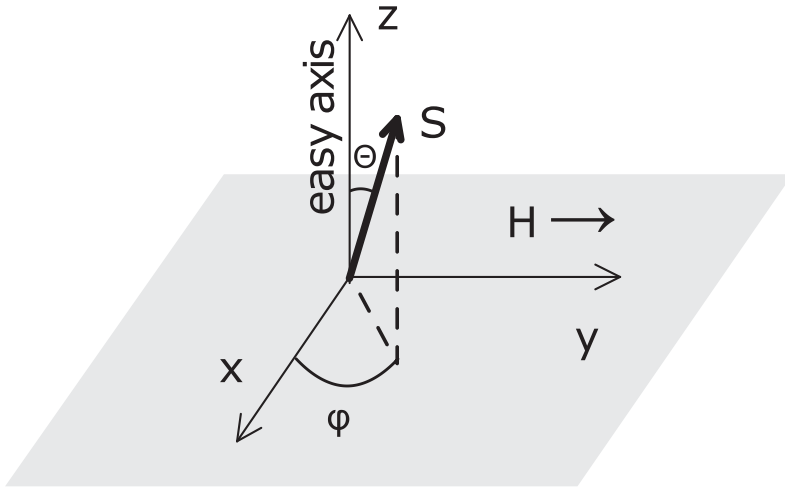


FIG. 5. Schematic representation of the considered wire-substrate model. The wire is placed along the x -axis, and a constant magnetic field is applied perpendicular to the wire.

constant of $K = 2.17$ meV and a magnetic moment μ of $\mu_s = 2.1\mu_B$ for the unstrained case. Using Eq. (5), we obtained the normalized value of the spin moment S_z projection on the easy-axis of magnetization as a function of the external magnetic field (H_y) strength. The solutions of Eq. (5) yield to two stable spin states: “up” and “down” ($S_z > 0$ and $S_z < 0$, respectively), see the solid lines in Fig. 6. Our results show a meaningful reduction of the magnetic moment with the increase of magnetic field strength for both spin states. For instance, in the case of an applied magnetic field of 30 T, the S_z reduces 30% of its value. Alongside, the increase of magnetic field leads to the increase of the magnetic spin moment precession velocity $\partial S_i / \partial t$ (see Eq. (1)) and energy. Thus, the magnetization reversal can be obtained upon the magnetic field $\mathbf{H} = \{0; H_y; 0\}$ exposure. The minimum magnetic field required for magnetization switching is proportional to the magnetic anisotropy energy in order to overcome the energy barrier between the two spin states. In the case of Co/Pt(111)

$$H_{switch} = \frac{K}{\mu_s} = 17.9 \text{ T}. \quad (6)$$

It should be noted, that such robust estimation is in good agreement with our numerical calculations performed via the

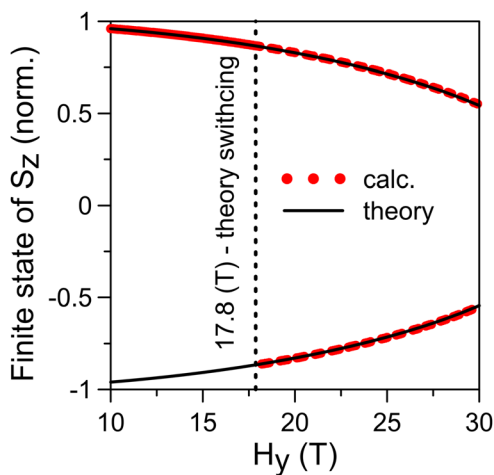


FIG. 6. Normalized magnetization projection of S_z onto the z -axis as a function of external magnetic field H_y for the Co/Pt(111) system.

Runge-Kutta fourth order method with $\Delta t = 10^{-16}$, $\alpha = 0.01$, $\Theta(0) = 0.01$, $\varphi(0) = \pi/2$ (Fig. 6, red points). We found that magnetization reversal occurs upon a magnetic field strength of $H_{switch} = 18.2$ T. The small difference between both (estimated and numerically calculated) values for H can be explained by the energy damping term. However, such estimations are applicable only for systems with ferromagnetic alignment between the atoms since the magnetization dynamics for antiferromagnetic systems is sensitive to the value of the inter-atomic exchange interaction.³⁹

In order to estimate the corresponding switching time, we have calculated the time-dependent evolution of the spin moment projection S_z as a function of the external magnetic field strength. We consider two magnetic field strengths— $H_y = 18.1$ T and $H_y = 18.2$ T—and found that the time-dependence of the magnetization projection of S_z qualitatively changes upon switching (Fig. 7). Additionally, one finds that the magnetization switching occurs in less than 2 ps upon the external magnetic field exposure.

Also it is possible to use magnetic pulses for inducing magnetization switching in nanosystems.³⁹ Using the method described in Ref. 39, we have examined the Co/Pt(111) system. Our calculations show that in the case of a magnetic field strength of $H = 18.2$ T, the pulse time required for

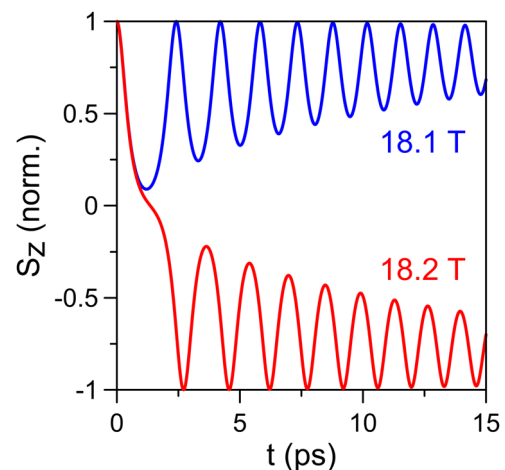


FIG. 7. Time-dependence evolution of the spin magnetic moment projection S_z for Co/Pt(111).

inducing magnetization switching is $t_{pulse} = 1.7$ ps; in the case of $H = 20$ T, the pulse time is $t_{pulse} = 0.6$ ps. In general, we observe that stronger magnetic fields lead to a decrease in the pulse times for inducing magnetization reversal.

Our analysis reveals that the critical magnetic field which is necessary for prompting magnetization switching in supported ferromagnetic coupled 1D wires, is proportional to the MA energy of the system (Eq. (6)). Since our first-principles calculation results show a significant monotonic decrease of the MA energy upon induced strain for deposited Co wires, we expect smaller switching magnetic fields for the case of strained systems in comparison to the corresponding non-strained ones. Our numerical calculations are in-line with the theoretical estimations predicted by the Stoner-Wohlfarth-like model and show that the induced surface-strain leads to a decrease of the magnetic field strength required for magnetization switching. Fig. 8 shows both the calculated and estimated critical magnetic field strengths needed for inducing magnetization reversal as a function of the substrate lattice parameter for Co/Pt(111). As one can see, our numerical results are in agreement with the estimations using phenomenological models.

For instance, a stretching of the lattice parameter around 2% reduces the MA energy from 2.2 to 0.5 meV. We observe a substantial decrease of the magnetic field strength for such strained system. The magnetization switching occurs when

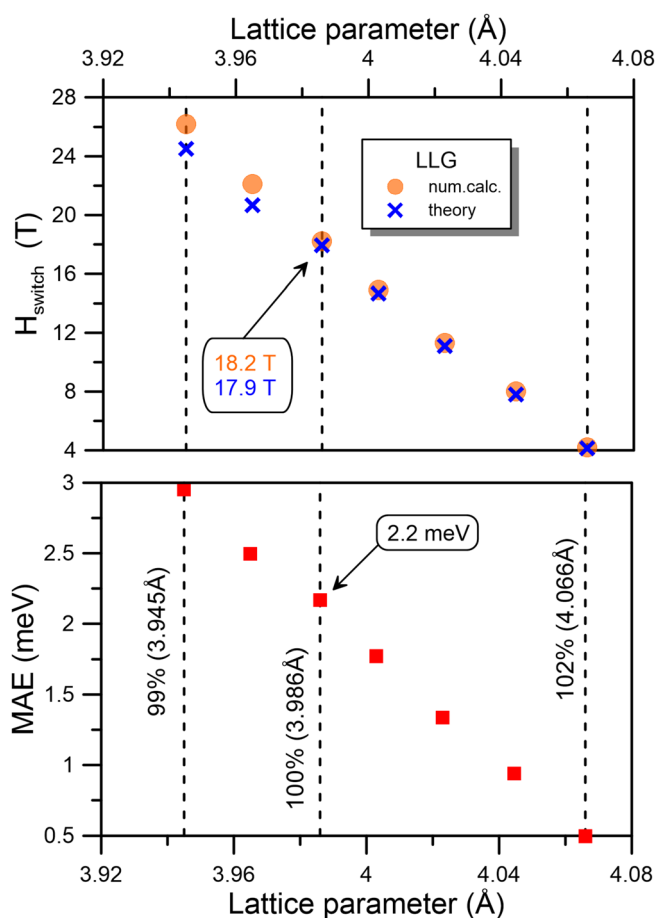


FIG. 8. (a) Critical magnetic switching field and (b) the MA energy as a function of the lattice parameter for Co/Pt(111).

the strength of the field is $H = 4$ T and is roughly 4.6 times smaller than the magnetic field for the corresponding non-strained system (18.2 T). A similar trend is observed for the case of Co/Au(111). We found a switching magnetic field of $H_{switch} = 4.0$ T and $H_{switch} = 2.0$ T for the non-strained and strained systems, respectively. In this case, the switching magnetic field decreases two times upon strain. In general, for both Co/Pt(111) and Co/Au(111) systems, we obtain a monotonous reduction of the anisotropy energy upon inducing the surface-strain which results in a decrease of the switching magnetic field strength.

IV. SUMMARY

Summarizing our results, in this work we have demonstrated that the surface-strain has a strong impact on the magnetic properties and the underlying magnetization dynamics of deposited metallic nanowires. In the case of Co wires on Pt(111) and Au(111) substrates, our first-principle calculations reveal that both compressive and tensile strains induce an electronic redistribution of d -states of the wires. This redistribution leads to a change in coupling between atoms in wire resulting in a monotonic increase/decrease of anisotropy energy under compressive/tensile surface strain.

The monotonic decrease of the anisotropy energy plays a crucial role in the magnitude of the external magnetic field H_{switch} required for magnetization switching. Our findings suggest as a first approach, that the switching magnetic field H_{switch} , can be estimated assuming that its value is directly proportional to the MA energy. We demonstrated that such estimated values H_{switch} are in good agreement with the results obtained upon solving the LLG equation. The reduction of the H_{switch} by means of induced surface-strain offers an alternative to decrease the demanded energy for magnetization reversal processes which are of great interest in the novel spintronic devices design in order to diminish their energy consumption.

ACKNOWLEDGMENTS

The authors thank Professor V. S. Stepanyuk for useful discussions. This study was supported by the Russian Foundation for Basic Research (Project No. 13-02-01322-a).

- ¹J. Dorantes-Dávila and G. M. Pastor, *Phys. Rev. Lett.* **81**, 208 (1998).
- ²D. S. G. Bauer, P. Mavropoulos, S. Lounis, and S. Blügel, *J. Phys.: Condens. Matter* **23**, 394204 (2011).
- ³P. Gambardella, M. Blanc, L. Bürgi, K. Kuhnke, and K. Kern, *Surf. Sci.* **449**, 93 (2000).
- ⁴H. J. Elmers, J. Hauschild, H. Höche, U. Gradmann, H. Bethge, D. Heuer, and U. Köhler, *Phys. Rev. Lett.* **73**, 898 (1994).
- ⁵J. Shen, R. Skomski, M. Klaua, H. Jenniches, S. S. Manoharan, and J. Kirschner, *Phys. Rev. B* **56**, 2340 (1997).
- ⁶J. Hauschild, H. J. Elmers, and U. Gradmann, *Phys. Rev. B* **57**, R677 (1998).
- ⁷M. Pratzner, H. J. Elmers, M. Bode, O. Pietzsch, A. Kubetzka, and R. Wiesendanger, *Phys. Rev. Lett.* **87**, 127201 (2001).
- ⁸P. Gambardella, A. Dallmeyer, K. Maiti, M. Malagoli, W. Eberhardt, K. Kern, and C. Carbone, *Nature* **416**, 301 (2002).
- ⁹R. Cheng, E. Ayieta, and Y. B. Losovyj, *J. Vac. Sci. Technol., A* **26**, 673 (2008).
- ¹⁰J. Korobova, D. Bazhanov, I. Kamynina, K. Abgaryan, and A. Ilyushin, *Phys. Solid State* **57**, 1366 (2015).

- ¹¹P. Gambardella, M. Blanc, H. Brune, K. Kuhnke, and K. Kern, *Phys. Rev. B* **61**, 2254 (2000).
- ¹²J. C. Tung and G. Y. Guo, *Phys. Rev. B* **76**, 094413 (2007).
- ¹³Q. Dubout, F. Donati, C. Wackerlin, F. Calleja, M. Etzkorn, A. Lehnert, L. Claude, P. Gambardella, and H. Brune, *Phys. Rev. Lett.* **114**, 106807 (2015).
- ¹⁴O. O. Brovko, D. I. Bazhanov, H. L. Meyerheim, D. Sander, V. S. Stepanyuk, and J. Kirschner, *Surf. Sci. Rep.* **69**, 159 (2014).
- ¹⁵D. Sander, C. Schmidhals, A. Enders, and J. Kirschner, *Phys. Rev. B* **57**, 1406 (1998).
- ¹⁶V. S. Stepanyuk, D. I. Bazhanov, A. N. Baranov, W. Hergert, P. H. Dederichs, and J. Kirschner, *Phys. Rev. B* **62**, 15398 (2000).
- ¹⁷S. C. Jain and W. Hayes, *Semicond. Sci. Technol.* **6**, 547 (1991).
- ¹⁸D. Sander, R. Skomski, A. Enders, C. Schmidhals, D. Reuter, and J. Kirschner, *J. Phys. D: Appl. Phys.* **31**, 663 (1998).
- ¹⁹D. Sander, *Rep. Prog. Phys.* **62**, 809 (1999).
- ²⁰P. Juszyński, M. Gryglas-Borysiewicz, J. Szczytko, M. Tokarczyk, G. Kowalski, J. Sadowski, and D. Wasik, *J. Magn. Magn. Mater.* **396**, 48 (2015).
- ²¹J. Zhou, Q. Wang, Q. Sun, Y. Kawazoe, and P. Jena, *Phys. Chem. Chem. Phys.* **17**, 17182 (2015).
- ²²P. V. Lukashev, N. Horrell, and R. F. Sabirianov, *J. Appl. Phys.* **111**(7), 07A318 (2012).
- ²³C. Ratsch, A. P. Seitsonen, and M. Scheffler, *Phys. Rev. B* **55**, 6750 (1997).
- ²⁴D. I. Bazhanov, I. V. Mutigullin, A. A. Knizhnik, B. V. Potapkin, A. A. Bagaturyants, L. R. C. Fonseca, and M. W. Stoker, *J. Appl. Phys.* **107**, 083521 (2010).
- ²⁵D. Pesquera, G. Herranz, A. Barla, E. Pellegrin, F. Bondino, E. Magnano, F. Sanchez, and J. Fontcuberta, *Nat. Commun.* **3**, 1189 (2012).
- ²⁶C. Aruta, G. Ghiringhelli, A. Tebano, N. G. Boggio, N. B. Brookes, P. G. Medaglia, and G. Balestrino, *Phys. Rev. B* **73**, 235121 (2006).
- ²⁷A. Tebano, C. Aruta, S. Sanna, P. G. Medaglia, G. Balestrino, A. A. Sidorenko, R. De Renzi, G. Ghiringhelli, L. Braicovich, V. Bisogni, and N. B. Brookes, *Phys. Rev. Lett.* **100**, 137401 (2008).
- ²⁸M. Huijben, L. W. Martin, Y.-H. Chu, M. B. Holcomb, P. Yu, G. Rijnders, D. H. A. Blank, and R. Ramesh, *Phys. Rev. B* **78**, 094413 (2008).
- ²⁹A. Tebano, A. Orsini, P. G. Medaglia, D. Di Castro, G. Balestrino, B. Freelon, A. Bostwick, Y. J. Chang, G. Gaines, E. Rotenberg, and N. L. Saini, *Phys. Rev. B* **82**, 214407 (2010).
- ³⁰Z. Fang, I. V. Solov'yev, and K. Terakura, *Phys. Rev. Lett.* **84**, 3169 (2000).
- ³¹P. Campiglio, V. Repain, C. Chacon, O. Fruchart, J. Lagoute, Y. Girard, and S. Rousset, *Surf. Sci.* **605**, 1165 (2011).
- ³²P. E. Blochl, *Phys. Rev. B* **50**, 17953 (1994).
- ³³G. Kresse and J. Furthmüller, *Phys. Rev. B* **54**, 11169 (1996).
- ³⁴We performed several test calculations with different k-meshes ($4 \times 16 \times 1$, $5 \times 20 \times 1$, $6 \times 24 \times 1$, $7 \times 28 \times 1$) and different energy-cutoffs (400, 500, 600 eV) and found that the chosen values yield in variations in the ground state energy smaller than 0.1 meV/atom.
- ³⁵H. J. G. Draaisma and W. J. M. de Jonge, *J. Appl. Phys.* **64**, 3610 (1988).
- ³⁶F. Muoz, J. Meja-Lpez, T. Prez-Acle, and A. H. Romero, *ACS Nano* **4**, 2883 (2010).
- ³⁷R. F. L. Evans, W. J. Fan, P. Chureemart, T. A. Ostler, M. O. A. Ellis, and R. W. Chantrell, *J. Phys.: Condens. Matter* **26**, 103202 (2014).
- ³⁸S. Bhattacharjee, A. Bergman, A. Taroni, J. Hellsvik, B. Sanyal, and O. Eriksson, *Phys. Rev. X* **2**, 011013 (2012).
- ³⁹K. Tao, O. P. Polyakov, and V. S. Stepanyuk, *Phys. Rev. B* **93**, 161412 (2016).
- ⁴⁰R. Wieser, V. Caciuc, C. Lazo, H. Hlscher, E. Y. Vedmedenko, and R. Wiesendanger, *New J. Phys.* **15**, 013011 (2013).
- ⁴¹O. P. Polyakov and V. S. Stepanyuk, *J. Phys. Chem. Lett.* **6**, 3698 (2015).
- ⁴²F. V. Lisovskii and O. P. Polyakov, *J. Exp. Theor. Phys. Lett.* **68**, 679 (1998).
- ⁴³We additionally performed further calculations with different time-steps ($\Delta t = 10^{-16}$ s), finding qualitatively the same results only with differences smaller than 1%.
- ⁴⁴M. Yan, J. Berezovsky, P. A. Crowell, and C. E. Campbell, in *Condensed Matter Theories*, edited by M. P. Das and F. Green (Nova, New York, 2003), Vol. 17, p. 295.
- ⁴⁵B. Skubic, J. Hellsvik, L. Nordstrm, and O. Eriksson, *J. Phys.: Condens. Matter* **20**, 315203 (2008).
- ⁴⁶*Symmetry, Spin Dynamics and the Properties of Nanostructures: Lecture Notes of the 11th International School on Theoretical Physics*, edited by V. Dugaev, A. Wal, and J. Barna (World Scientific Publishing, Singapore, 2015).
- ⁴⁷*Spin Dynamics in Confined Magnetic Structures II*, edited by B. Hillebrands and K. Ounadjela (Springer Science & Business Media, 2003).
- ⁴⁸K. Roy, S. Bandyopadhyay, and J. Atulashimha, *Appl. Phys. Lett.* **99**, 063108 (2011).
- ⁴⁹O. Gunnarsson, O. K. Andersen, O. Jepsen, and J. Zaanen, *Phys. Rev. B* **39**, 1708 (1989).
- ⁵⁰P. Wahl, A. P. Seitsonen, L. Diekhner, M. A. Schneider, and K. Kern, *New J. Phys.* **11**, 113015 (2009).
- ⁵¹S. Bornemann, O. Šipr, S. Mankovsky, S. Polesya, J. B. Staunton, W. Wurth, H. Ebert, and J. Minar, *Phys. Rev. B* **86**, 104436 (2012).
- ⁵²D.-S. Wang, R. Wu, and A. J. Freeman, *Phys. Rev. B* **47**, 14932 (1993).
- ⁵³T. R. Dasa, P. A. Ignatiev, and V. S. Stepanyuk, *Phys. Rev. B* **85**, 205447 (2012).
- ⁵⁴P. Ruiz-Dıaz, O. V. Stepanyuk, and V. S. Stepanyuk, *J. Phys. Chem. C* **119**, 26237 (2015).
- ⁵⁵W. Kohn, *Rev. Mod. Phys.* **71**, 1253 (1999).
- ⁵⁶H. J. Monkhorst and J. D. Pack, *Phys. Rev. B* **13**, 5188 (1976).